doi:10.14311/ppt.2025.2.130
Plasma Physics and Technology **12**(2):130–135, 2025

MEDIUM VOLTAGE DIRECT CURRENT INTERRUPTION BY A HIGH VELOCITY FLOW OF DIELECTRIC LIQUIDS

S. Jugelt[a,*], C. Leu[b]

[a] *Research Unit High-Voltage Technologies, Technische Universität Ilmenau, Gustav-Kirchhoff-Straße 1, 98693 Ilmenau, Germany*

[b] *Electrical Power Systems and High-Voltage Engineering, HTWK Leipzig University of Applied Sciences, Wächterstraße 13, 04107 Leipzig, Germany*

[*] stefan.jugelt@tu-ilmenau.de, carsten.leu@htwk-leipzig.de

Abstract. The increasing availability of self-sufficient MVDC systems necessitates innovative MVDC switching solutions. Direct current interruption is achieved by inducing a current zero and preventing re-ignition. In addition to complex resonant networks that create oscillating currents with natural current zeros, another method uses a switching device that generates an arc voltage higher than the grid voltage for current limiting. Conventional gas or vacuum interrupters fail at higher voltages. This paper builds upon previous investigations on the contact separation in dielectric liquids for MVDC interruption. A low inertia mass contact mechanism is used and measurements are carried out for 50 A to 250 A direct current interruption at 10 kV. The study investigates the switching performance of synthetic ester and synthetic oil.

Keywords: MVDC interruption, switching arc in liquids, current limiting.

1. Introduction

The advancement of high-voltage power electronics has enabled innovative multi-terminal MVDC electrical grid topologies [1]. However, the implementation of high and medium voltage direct currents poses challenges in current interruption due to the absence of a natural current zero crossing, making AC switchgear technologies inapplicable [2]. Three primary principles address this: divergent oscillation and current injection, using synthetic resonant networks with ultra-fast disconnectors or main circuit breakers, and the creation of a voltage above the grid voltage through an electric arc or semiconductor circuit, forcing the current to zero (current limiting principle). The arc voltage (V_{arc}) can be expressed as $V_{\mathrm{arc}} = V_{\mathrm{a}} + E_{\mathrm{arc}} l_{\mathrm{arc}} + V_{\mathrm{c}}$, where E_{arc} is the voltage gradient of the arc column, V_{a} the anode voltage drop, and V_{c} the cathode voltage drop. Various methods contribute to the rapid increase of the arc voltage and which can also be employed in combination:

- electrodes that diverge to employ the Lorentz force for the purpose of inducing a movement of the arc [3], thereby extending the arc column l_{arc};
- the quenching of the arc within narrow gaps [4], thereby extending the length of the arc column l_{arc} and correspondingly elevating the voltage gradient of the arc column E_{arc};
- increasing the cooling of the arc through the evaporation of an insulating material [5], a process that also results in an increase in pressure, thereby enhancing the voltage gradient E_{arc}

During arc motion, the increase in voltage may be constrained by various factors. Firstly, the rising arc voltage can lead to thermal and dielectric breakdowns in the surrounding gas (back-commutation) [6], which reduces the arc length and results in a diminished mean arc velocity. Moreover, variations in electromagnetic and hydrodynamic forces exerted on the arc contribute to unstable and decelerated arc movement [7]. Both phenomena impede the elevation of the arc voltage and can potentially lead to unsuccessful current interruption. Despite extensive research conducted on these issues, a comprehensive solution has yet to be established. In light of this, it appears feasible to investigate new methodologies for increasing the arc voltage of direct current arcs, in conjunction with current limitation, with the goal of achieving current zero.

Gerdien [8] initially demonstrated that an electric arc immersed in a steady flow of water exhibits a significantly higher rate of power dissipation compared to ambient air. This finding was later explored by Ann [9] and Möllenhoff [10], who employed a forced oil flow perpendicular to the electric arc to illustrate a rapid increase to very high arc voltages (~ 70 kV) by rapidly extending the arc length. The very fast elongation of the arc prevents the build up of an extended vapor phase, which would decrease the arc cooling and thus limit the arc voltage increase as well as the dielectric strength of the fluid.

Based on the hypothesis that enhanced arc voltages result from an induced fluid flow of a dielectric liquid, prior exploratory measurements [11] demonstrated the potential for a current limiting application and consequently direct current interruption for several kilovolts. This paper extends the previous

research [11, 12] with particular interest on dielectric liquids with high molecular hydrogen content but varying molecular structures. This study focuses on synthetic oil (Shell Diala S4, presumed $C_{18}H_{38}$) and synthetic ester (Midel 7131, presumed $C_{25}H_{44}O_8$).

Currently, there are no standardized grid voltage levels available for practical application and subsequent research. Therefore, it is essential to utilize the MVDC distribution grid levels proposed by Cigré [1] as constraints for this study. This work targets the "medium voltage level" (10 kV) due to the constraints in voltage and power of the available test circuit. The focus is on the application of nominal power-limited DC sources within multi-terminal MVDC grids, where all components are connected to the DC link via power converters. AC-side feed-through fault currents are not considered in this investigation.

2. Theoretical Background

2.1. Current Limiting

The principle of current limiting in DC applications can be explained from the simple network model in Fig. 1.

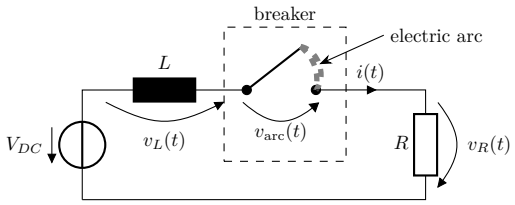

Figure 1. Simplified DC grid

In order to achieve a current zero condition, the arc voltage must exceed both the source voltage (V_{DC}) and the transient inductive voltage (V_L, as $^{di}/_{dt} < 0$), as described in Eq. (1).

$$V_{\text{arc}} \geq V_{DC} - v_L - i\,R \tag{1}$$

Assuming that the voltage drops across the anode and cathode are negligible for the required high voltages, the arc voltage can be approximated by $V_{\text{arc}} \approx E_{\text{arc}} l_{\text{arc}}$. Furthermore, considering that the arc elongates at a constant velocity, the arc voltage can be expressed as $V_{\text{arc}} \approx E_{\text{arc}} v_{\text{arc}} t$. Assuming there are no transient currents within the grid prior to the operation of the breaker ($i(t \leq 0) = I_{DC} = {}^{V_{DC}}/_{R}$), solving Eq. (1) yields:

$$\frac{i}{I_{DC}} = 1 - \frac{E_{\text{arc}} v_{\text{arc}}}{V_{\text{DC}}} \left\{ t - \frac{L}{R} \left[1 - exp\left(-\frac{R}{L} t \right) \right] \right\} \quad . \tag{2}$$

It is evident from Eq. 2 that the electrical network is characterized by a time constant $\tau = {}^{L}/_{R}$. By solving Eq. (2) for the condition of current zero $i(t_{\text{arc}}) = 0$ and simplifying the exponential function, the arcing time can be determined as follows:

$$t_{\text{arc}} \approx \sqrt{\frac{2\,V_{DC}}{E_{\text{arc}} v_{\text{arc}}} \tau} \quad . \tag{3}$$

2.2. Heat transfer from the arc

To initiate an electric arc within a liquid, the generation of vapor (gas) is required first. The heat produced by the current-carrying metal vapor arc, which occurs after contact separation, acts on the surrounding liquid. This causes the boundary layer of the liquid to be heated to its boiling point. Beyond this point, additional thermal energy is not converted into further heating of the liquid. Instead, it is used to overcome the intermolecular forces within the liquid, characterized by the enthalpy of vaporization (Δh_V). Values of Δh_V for the liquids investigated here can be found in [13, 14]

Due to the steep temperature gradient in the vapor phase, radiation is nearly entirely absorbed within the vapor. Consequently, the mass transfer from liquid to vapor can be approximated by linear heat conduction ($\mathbf{q} = -k\nabla T$) at the phase boundary as:

$$S_q = -\dot{m}_{lv} \Delta h_v = \nabla \cdot (\mathbf{q}_v - \mathbf{q}_l) \tag{4}$$

the sum of the heat absorbed by the liquid ($\mathbf{q}_l = k_l \nabla T_l$) and the heat transferred to the phase boundary through the vapor ($\mathbf{q}_v = k_v \nabla T_v$).

Based on the molecular composition of the liquid phase, the material properties of the vapor phase were approximated using the program CEA [15] assuming an equilibrium composition. It should be noted that only first-order ionization states can be calculated, so above approximately 15 000 K, the values are inaccurate. Furthermore, occurring solid carbon particles are not taken into account. The calculated transportation and thermodynamic parameters are given in Fig. 2 for ambient pressure.

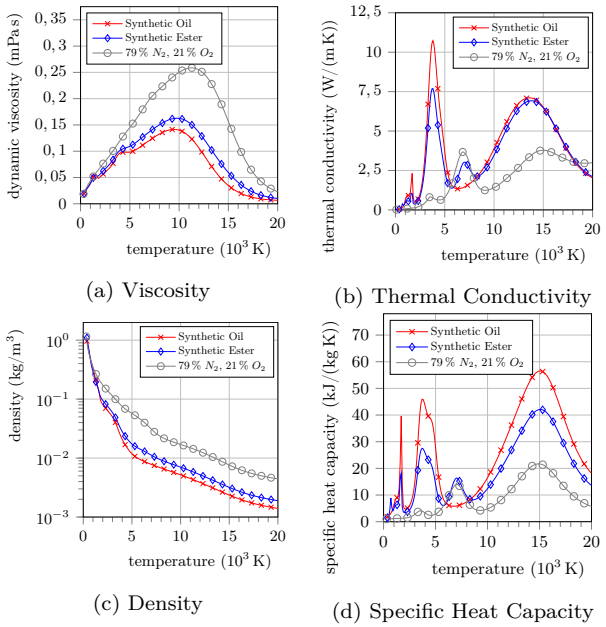

(a) Viscosity (b) Thermal Conductivity

(c) Density (d) Specific Heat Capacity

Figure 2. Material properties of the evaporated liquids (gas phase) [15] in comparison with air [16]

Approximately 60 % (Ester) / 70 % (Oil) of the dissociated vapor consists of hydrogen. Due to the low

collision cross-section of hydrogen ions, the mean free path length is relatively high, resulting in significantly enhanced thermal conductivity (approximately an order of magnitude higher than air) and specific heat capacity (nearly two orders of magnitude higher than air) of the vapor compared to other gases like air, see Fig. 2. This leads to a substantial cooling effect on the electric arc, thereby significantly increasing the voltage gradient of the arc column (E_{arc}).

3. Experimental Setup

3.1. Electrical Test Circuit

Testing HVDC interruption presents significantly greater challenges compared to HVAC, as the requisite test circuit must simultaneously supply high voltage and high current, resulting in exceptionally high testing power requirements. To address this, a synthetic test circuit was constructed. This circuit employs a pulse forming network (PFN) configured in a lattice arrangement of capacitors (C_0) and inductors (L_0). A comprehensive description can be found in [17]. The capacitors are charged to the test voltage ($V_0 = 10\,\mathrm{kV}$) and subsequently, the PFN is discharged into the device under test (DUT). When the load resistance (R_L) matches the line impedance of the PFN ($Z_0 = \sqrt{L_0/C_0}$), the PFN generates a direct current pulse with an amplitude of approximately 1000 A and a duration of 25 ms. For this investigation, the resistance R_L was adjusted to achieve the desired test currents in the range of 50 A to 250 A ($R_L = 200\,\Omega$ to $33\,\Omega$).

3.2. Switching Apparatus

As demonstrated in previous research [9, 10], it is essential to direct the fluid flow towards the electric arc, in contrast to separating electrodes within a liquid flow. Furthermore, achieving the high arc voltages necessary for high voltage direct current interruption by current limiting requires a rather high flow velocity. In our test setup, a modified pneumatic piston pump is utilized to accelerate the liquid. The pneumatic piston is pre-charged to a specific pressure and equipped with an electrically triggerable locking mechanism. This mechanism ensures that the acceleration of the pneumatic piston is constrained only by the inertia of the piston and the mass of the fluid within the switching apparatus. Consequently, a constant flow velocity of the liquid is rapidly attained and maintained for approximately 10 milliseconds. Assuming the liquid is incompressible, a high fluid flow velocity is generated by reducing the cross-sectional area of the cylindrical channel of the piston pump, as illustrated in Fig. 3. The piston's position along its axis is monitored using a laser triangulation sensor, enabling the calculation of the liquid's volumetric flow rate.

Above the piston pump, contacts are arranged in a 90° V-shape, forming a divergent electrode configuration that leverages the Lorentz force to propel the arc upward once the contacts separate. The fluid flow itself initiates this process, facilitated by a flow channel beneath the contacts that directs the fluid onto a propulsion disc mounted on the contacts. As the contacts begin to move, they overcome the tension of an attached bistable spring. This bistable spring ensures contact force in the closed position and maintains separation in the open position.

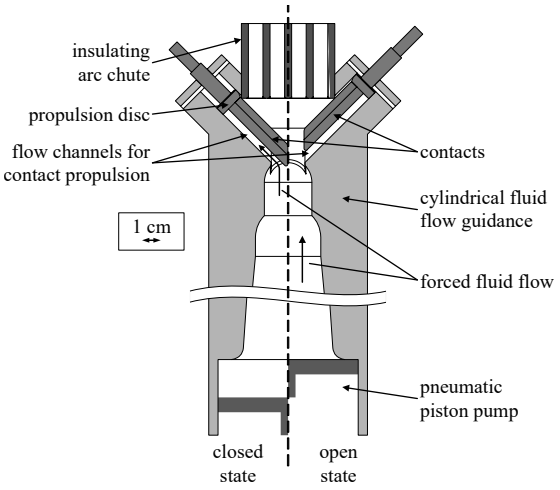

Figure 3. Cross section view of the direct current interruption apparatus

To achieve a rapid increase in arc voltage, the arc column length must also rapidly increase. This is most effectively accomplished by directing the arc into narrow channels, resulting in a length increase that is double the physical movement of the arc. This concept is applied here using a insulating arc chute made from polymer (POM). No significant ablation of the material was observed during the measurements.

Previous measurements indicated that with increasing fluid flow velocity, the dielectric breakdown strength of the dielectric liquid decreases due to cavitation effects [12]. Therefore, for the design of the insulating arc chute, a maximum fluid flow velocity of $25\,\mathrm{m\,s^{-1}}$ within the grid was established. Based on the known velocity of the piston pump at different pressures and the geometric dimensions of the piston pump, three arc chutes with varying numbers of openings (vents) were utilized, as shown in Fig. 4 and Tab. 1. These gratings were designed to maintain a consistent open space cross-section across all configurations, resulting in equal fluid flow velocities but differing arc length increases due to the multiple number of vents.

Configuration	Number of vents	B (mm)	T (mm)
4VT	4	7.8	7.5
6VT	6	5.2	7.5
8VT	8	3.9	7.5

Table 1. Dimensions of the various arc chutes ($B_{tot} = 50\,\mathrm{mm}$, $H = 40\,\mathrm{mm}$)

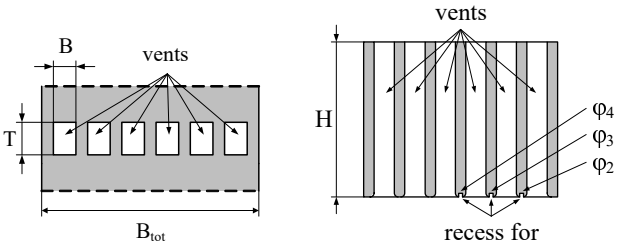

(a) top view

(b) section view

Figure 4. Insulating arc chute

To prevent electrical breakdown of the liquid, it is essential to uniformly increase the arc length across the multiple vents. To verify this, recesses for potential probes have been incorporated at the inlet edge of the vents, enabling the measurement of the electric arc's voltage distribution during current interruption.

4. Results

4.1. Typical Breaking Waveforms

Fig. 5 illustrates typical waveforms of arc voltage and current for a 250 A direct current interruption at a test voltage of 10 kV in synthetic ester (Fig. 5a) and synthetic oil (Fig. 5b). The mean fluid velocity is inferred as the liquid velocity within the vents, calculated based on piston movement and the reduction in geometrical cross-section.

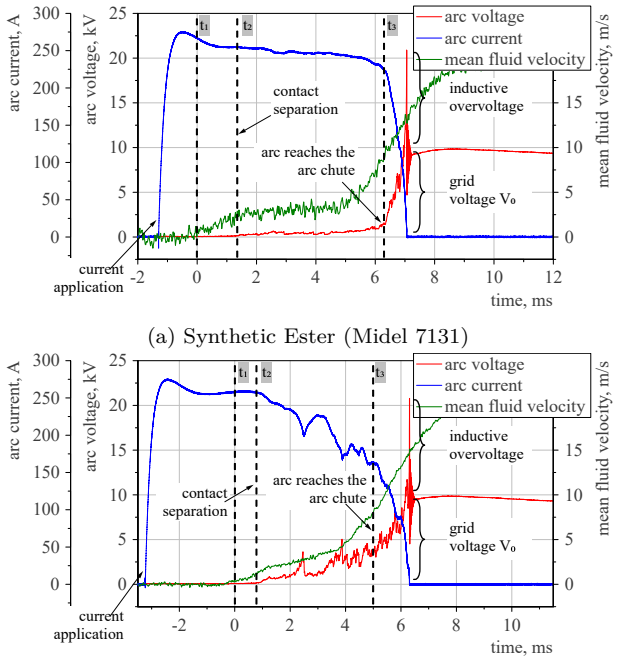

(a) Synthetic Ester (Midel 7131)

(b) Synthetic Oil (Shell Diala S4)

Figure 5. Exemplary measurements for 250 A direct current interruption

For our measurements, the onset of the current interruption process is defined by a piston movement of 250 µm along its axis (time t_1), as the exact instant of contact separation (t_2) cannot be precisely determined by the voltage measurement (the anode and cathode voltage drops are approximately 100 V, are relatively low compared to the maximum measured voltages of up to 25 kV). With the arc burning in the vapor bubble of the liquid, a slight voltage increase can be observed after t_2 due to the cooling effect of vaporization, which is limited by the small surface area of the arc. Upon the arc reaching the arc chute (t_3), detected by the potential probes, the arc voltage sharply increases as the arc is quenched at the edges of the vents and subsequently elongated into the vents, rapidly expanding the vapor-liquid interface (vaporization area). Owing to the inductance of the test circuit, a high inductive overvoltage is recorded in the time domain of current zero.

4.2. Voltage distribution

One of the main disadvantages of conventional (minimal) oil circuit breakers is the non-uniform voltage distribution across the vents due to time dependent linear uncovering of them. With our modified contact arrangement, the fluid flow should evenly reach all vents at the same time. This can be validated by evaluation of the differential voltages of the potential probes at the edges of the vents. The differential voltages are defined as (see also Fig. 4b).

$$\Delta V_1 = V_{in} - \varphi_2 \,,\; \Delta V_2 = \varphi_2 - \varphi_3 \,,\; \Delta V_3 = \varphi_3 - \varphi_4 \quad (5)$$

Fig. 6 gives the differential voltages of selected measurements for different arc chutes and synthetic ester used as dielectric liquid. Due to the limited DSO measurement channels, only the high voltage side of the apparatus is measured. The fluid flow is assumed to be mirror symmetrical. The waveforms validate the assumption of a uniform voltage distribution across the vents.

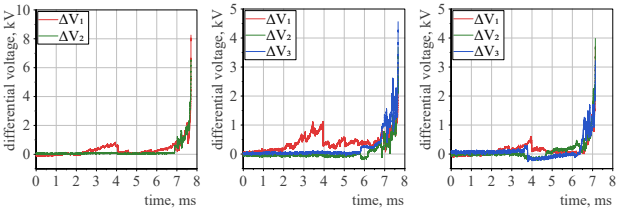

(a) 4VT (b) 6VT (c) 8VT

Figure 6. Differential voltages of different arc chutes in synthetic ester for configurations

With the measured differential voltages and the known vent width (B), a maximum theoretical field strength at the instant of arc extinction can be approximated, see Tab. 2, considering that the maximum dielectric stress on the liquid is at the edge of the vents. It can be seen, that not only does the differential voltage decrease with increasing number of vents due to multiple arc sections, but also does the absolute value of the field strength decrease as well. Hence, there is

less dielectric stress on the dielectric liquid at high arc voltages, preventing breakdown (back-commutation) and so increased switching times. It is assumed to correlate with a decreased penetration depth of the arc into the vents, but needs further validation, we have not done yet.

Configuration	max. differential voltage	max. electric field strength
4VT	8.0 kV	10.3 kV cm^{-1}
6VT	4.5 kV	8.7 kV cm^{-1}
8VT	3.5 kV	8.9 kV cm^{-1}

Table 2. Maximum electric field strength at the edge of the vents for the measurements of Fig. 6 at instant of arc extinction

4.3. Arcing Time

In contrast to AC current interruption, arcing time in DC current interruption is not constrained by a natural current zero and is solely dependent on the switching capability of the interrupter. Therefore, the time to achieve current zero is of paramount importance. In this context, the arcing time is defined from t_1 to current zero. The time delay of the locking mechanism (approximately 10 ms) is not included.

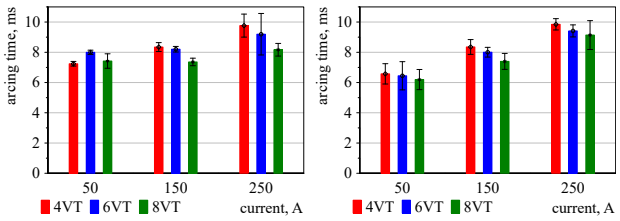

(a) Synthetic Ester (Midel 7131)

(b) Synthetic Oil (Shell Diala S4)

Figure 7. Arcing time for different currents and liquids

Fig. 7 presents the mean arcing times for ten measurements each. It can be observed that with increasing direct current to be interrupted, the arcing time also increases. This outcome is expected, as the theoretical arcing time (Eq. (3)) follows the increasing time constant of the DC circuit ($\tau = {}^{L}/_{R}$) in a degressive manner. Notably, the arcing time decreases with an increasing number of vents in the arc chutes. According to Eq. (3), this indicates enhanced field strength within the arc due to intensified arc cooling in narrower vents and faster arc elongation. When comparing Fig. 7a and Fig. 7b, it is evident that there are no significant differences in the arcing times between the two liquids for comparable currents. Considering that the fluid velocity for synthetic oil is higher than that for synthetic ester, this suggests a lower (mean) arc field strength for synthetic oil compared to synthetic ester.

4.4. Power Dissipation while Current Limiting

In the absence of a parallel dissipation path in current limiting circuit breakers, the input power from the electrical source must be absorbed by the arc. This is illustrated by the current-voltage and current-power characteristics shown in Fig. 8 for the measurements depicted in Fig. 5a.

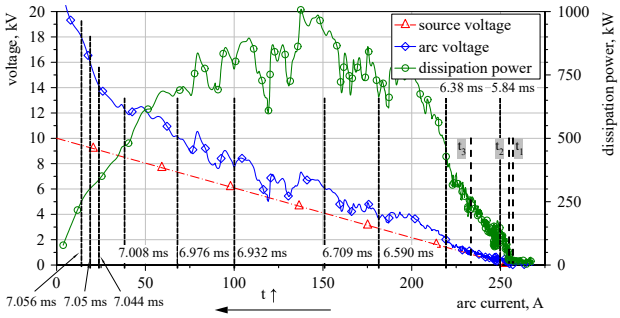

Figure 8. Arc voltage and dissipation power as in Fig. 5a

At every instant in time, the arc voltage is the sum of the source voltage ($V_{DC} - iR$) and the inductive voltage (V_L) as described in Eq. (1). The arc voltage increases almost linearly with current, resulting in a relatively low current decline (${}^{di}/_{dt}$) and thus a minor additional voltage (V_L), except during the final microseconds when the arc depletes completely due to the sharply increasing V-I characteristic of low current arcs. This behavior is validated by the current-power curve, where the maximum power point is observed at approximately half of the nominal current. The maximum power point can be derived from Eq. (1) under the assumption that ${}^{dP}/_{di} = 0$. The current

$$I_{P_{max}} = \frac{V_{DC}}{2R} - \frac{L}{2R}\left.\frac{di}{dt}\right|_{t=t(P_{max})} \tag{6}$$

is defined by the source (first term) and the gradient of the current decline at the maximum power point (second term). Consequently, increasing the current limiting (${}^{di}/_{dt} \uparrow$) shifts the maximum power point to higher currents and higher power. Fig 9 illustrates the evaluation of the maximum power point from the conducted measurements, providing an assessment of the rate of current decline.

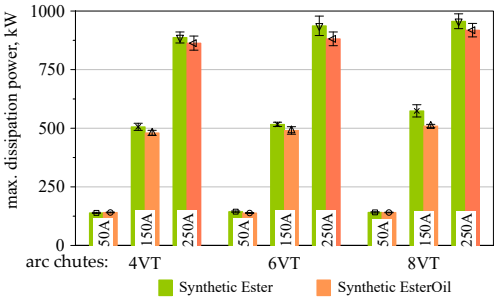

Figure 9. Maximum power dissipation in the electric arc during successful current interruption

It is notable that with an increasing number of vents, the maximum dissipation power also increases, which corresponds to an expected increase in current decline, as confirmed by lower arcing times. Furthermore, there is a significantly lower power dissipation observed for synthetic oil compared to ester. This is attributed to a lower current decline (in comparison to synthetic ester), as observed in Fig. 5a and Fig. 5b. However, this slower current decline results in a substantially increased arcing energy.

5. Conclusion

A self-developed DC switching apparatus has been investigated for medium voltage direct current interruption. The current interruption is achieved through current limiting, utilizing a forced flow of dielectric liquids. The liquids used are common dielectric insulation liquids (Shell Diala S4 and Midel 7131), chosen for their high molecular hydrogen content, which provides effective arc cooling in the vapor phase. The liquid flow is generated by a high-velocity pneumatic piston pump acting on the liquid, which forces the electric arc into an insulating arc chute. To study its DC interruption characteristics, breaking tests were accomplished under different currents in a DC test system consisting of a high voltage pulse forming network.

From the investigations, several conclusions can be drawn:

1. With the V-shape arrangement of the contacts and the perpendicular fluid flow, a uniform voltage distribution along the vents is achieved. This is important to avoid dielectric breakdown of the liquid and thus back-commutation of the arc due to the high arc voltages reached.

2. Measurements indicate that the arcing time decreases with an increasing number of vents in the insulating arc chutes. This is attributed to both an increased electric field strength within the arc due to enhanced arc cooling and faster arc elongation with a higher number of vents.

3. Evaluation of the peak electrical input power dissipated into the arc also reveals differences among the liquids. Throughout the measurements, synthetic oil exhibited lower maximum power dissipation.

References

[1] WG C6.31. Medium voltage direct current (MVDC) grid feasibility study. Technical report, Cigré, 2020.

[2] C. Meyer, M. Kowal, and R. W. De Doncker. Circuit breaker concepts for future high-power DC-applications. In *Fourtieth IAS Annual Meeting. Conference Record of the 2005 Industry Applications Conference*, volume 2, pages 860–866, 2005. doi:10.1109/IAS.2005.1518439.

[3] C. W. Brice, R. A. Dougal, and J. L. Hudgins. Review of technologies for current-limiting low-voltage circuit breakers. *IEEE Transactions on Industry Applications*, 32(5):1005–1010. doi:10.1109/28.536858.

[4] M. Lindmayer and Z. Huang. Current limiting switching by squeezing arcs into narrow insulating slots. *IEEE Transactions on Components, Hybrids, and Manufacturing Technology*, 15(2):160–165, April 1992. doi:10.1109/33.142889.

[5] P. Hettwer. Arc-interruption and gas-evolution characteristics of common polymeric materials. *IEEE Transactions on Power Apparatus and Systems*, PAS-101(6):1689–1696, June 1982. doi:10.1109/tpas.1982.317220.

[6] C. Fievet, M. Barrault, P. Chevrier, and P. Petit. Experimental and numerical studies of arc restrikes in low-voltage circuit breakers. *IEEE Transactions on Plasma Science*, 25(5):954–960, 1997. doi:10.1109/27.649604.

[7] R. Ma, M. Rong, F. Yang, et al. Investigation on arc behavior during arc motion in air dc circuit breaker. *IEEE Transactions on Plasma Science*, 41(9):2551–2560, September 2013. doi:10.1109/tps.2013.2273832.

[8] H. Gerdien and A. Lotz. Über eine lichtquelle von sehr hoher flächenhelligkeit. In *Wissenschaftliche Veröffentlichungen aus dem Siemens-Konzern*, volume 2, pages 489–496. Julius Springer, 1922.

[9] H. Ann. *Untersuchungen über die Erzeugung sehr hoher Lichtbogenspannungen unter Flüssigkeiten*. PhD thesis, TH Braunschweig, 1966.

[10] K. Möllenhoff. *Untersuchungen zur Entwicklung eines Lichtbogen-Ölströmungsschalters für die Hochspannungs-Gleichstrom-Übertragung*. PhD thesis, Technische Universität Carolo-Wilhelmina zu Braunschweig, 1968.

[11] S. Jugelt and C. Leu. Interruption of medium-voltage direct-currents by seperation of contact elements in mineral oil using an ultra fast electro-magnetic actuator. *Plasma Physics and Technology*, 6(1):73–77, 2019. doi:10.14311/ppt.2019.1.73.

[12] S. Jugelt and Y. Geng. Influence of liquid flow velocity on the breakdown characteristics of dielectric fluids in quenching gaps. In *21st International Conference on Dielectric Liquids (ICDL)*, Sevilla, Spain, 2022. IEEE. ISBN 978-1-6654-8491-6. doi:10.1109/icdl49583.2022.9830927.

[13] J. Rumble. *CRC handbook of chemistry and physics : a ready-reference book of chemical and physical data*. CRC Press/Taylor & Francis Group.

[14] J. Muslim. *Study of dielectric liquids as alternative encapsulant for high temperature electronics power modules applications*. PhD thesis, Université Grenoble Alpes, 2019.

[15] S. Gordon and B. J. McBride. *Computer program for calculation of complex chemical equilibrium compositions and applications. Part 1: Analysis*.

[16] C. Rümpler. *Lichtbogensimulation für Niederspannungsschaltgeräte*. PhD thesis, Technische Universität Ilmenau, 2009.

[17] C. Drebenstedt, S. Jugelt, and M. Rock. Test circuit for evaluation of physical characteristics of SPDs with combined DC and impulse load. In *36th International Conference on Lightning Protection (ICLP)*, pages 608–613, Cape Town, South Africa, October 2022. IEEE. doi:10.1109/ICLP56858.2022.9942507.